

ORDERED ARRAYS OF Ca^{2+} -ATPase ON THE CYTOPLASMIC SURFACE OF ISOLATED SARCOPLASMIC RETICULUM

DONALD G. FERGUSON,* CLARA FRANZINI-ARMSTRONG,[‡] LORIANA CASTELLANI,[‡]
PETER M. D. HARDWICKE,[†] AND LINDA J. KENNEY[†]

*Departments of *Biology, [‡]Anatomy and [†]Physiology, University of Pennsylvania, Philadelphia, Pennsylvania 19104; [‡]Rosenstiel Basic Medical Sciences Research Center and [†]Department of Biology, Brandeis University, Waltham, Massachusetts 02254*

ABSTRACT Isolated sarcoplasmic reticulum (SR) vesicles with polymerized calcium pump protein were freeze-dried and rotary shadowed following uranyl acetate stabilization. This technique allows direct observation of a single side of the vesicle without requiring optical filtering. The heads of individual ATPase molecules, projecting above the cytoplasmic surface, are clearly resolved in the replicas. Ca ATPase molecules form extensive arrays in vanadate-treated, rabbit SR vesicles and in gently isolated, native SR vesicles from scallop. Gentle isolation results in limited areas of orderly structure in native SR isolated from vertebrate muscles. Special attention is given to the effect of various shadow thicknesses on the appearance of the heads. This information is essential to the interpretation of images in the accompanying paper (Franzini-Armstrong, C., and D. J. Ferguson, 1985, *Biophys. J.*, 48:607–615).

INTRODUCTION

The sarcoplasmic reticulum (SR) membrane contains a high concentration of a Ca-dependent ATPase, responsible for actively pumping calcium ions (see Martonosi and Beeler, 1983, for a review). The calcium pump protein is a single polypeptide of 100–110,000 mol wt (MacLennan, 1970; Meissner and Fleischer, 1971; Racker, 1972), asymmetrically inserted in the membrane and exposed on the cytoplasmic surface (Hasselbach and Elfvin, 1967; MacLennan et al., 1971; Inesi and Scales, 1974; Hidalgo and Ikemoto, 1977). The projections of the protein above the cytoplasmic surface of the membrane are at least 5 nm in length (Ikemoto et al., 1968; Dupont et al., 1973; Stewart and MacLennan, 1974; Hardwicke and Green, 1974; Jilka et al., 1975; Scales and Inesi, 1976; Herbet et al., 1977; Saito et al., 1978; Blaisie et al., 1982; Brady et al., 1982). The cytoplasmic projections (heads) of the ATPase are accessible to trypsin digestion, and comparison of tryptic fragments with sequenced portions of the molecules indicates that two short and one long segment of the molecule extend into the cytoplasm (Farley, 1983; see Moller et al., 1982, for a review).

The disposition of the molecules in the plane of the membrane and the size of the domain occupied by a single polypeptide and its accompanying lipids are less clearly understood. Evidence for some degree of polymerization has accumulated from a variety of experimental approaches (see Ikemoto, 1982 and Moller et al., 1982 for reviews). When solubilized in low concentrations of deter-

gent, the ATPase is in polymers of variable sizes (Le Maire et al., 1976; Dean and Tanford, 1977; Moller et al., 1980), indicating a natural tendency of the lipid-inserted ATPase to form aggregates. Other indirect evidence comes from electron microscopy. In freeze-fractured SR membranes the density of intramembranous particles is much less than the density of ATPase, as calculated from the extent of phosphorylation and from the size and spacings of the stain excluding regions on the surface of negatively stained SR vesicles (Jilka et al., 1975; Scales and Inesi, 1976; Wang et al., 1979). From this it is estimated that intramembranous particles represent aggregates of 2–4 polypeptides. Even though the intramembranous particles are strongly indicative of aggregation, these studies have not precisely determined the size of the presumptive oligomer, or solved the related problems of monomer domain size and of ATPase content in the membrane.

Considerable progress has been recently achieved with the study of orderly aggregates of Ca ATPase that have been either induced by vanadate (Dux and Martonosi, 1983a and b), or found in native SR from a scallop muscle (Castellani and Hardwicke, 1983). Filtered images from micrographs of negatively stained vesicles (Castellani and Hardwicke, 1983; Taylor et al., 1984; Buhle et al., 1983, 1984; Castellani et al., 1985) establish a dimeric basis for the ordered arrays, and allow calculation of the size of the minimum domain occupied by an individual polypeptide.

In this paper we use orderly arrays of ATPase to establish a correlation between the position of individual ATPase heads over the surface of SR vesicles, as seen in

high resolution shadow-cast images, and the position of stain-excluding regions in filtered images of negatively stained vesicles, as shown in the literature. An aspect of this study is a careful evaluation of the effects of variable shadow thicknesses on the appearance of orderly ATPase arrays. This information is crucial for the understanding of the distribution and density of the ATPase molecules in the more common disorderly arrangement found in native vertebrate SR (Franzini-Armstrong and Ferguson, 1985). We also detect the infrequent occurrence of ordered ATPase disposition in SR that have been gently isolated from skeletal muscle fibers of two vertebrates.

MATERIALS AND METHODS

Crude SR fractions were isolated from predominantly white, hind leg skeletal muscles of New Zealand white rabbits as described in Herbet et al., 1977.

Ordered arrays of Ca ATPase were produced in the rabbit SR using Na orthovanadate (Dux and Martonosi, 1983a). Several different procedures were used. Good results were obtained by dialyzing (Buhle et al., 1984) SR vesicles (1 mg protein/ml) suspended at pH 7.0 in 10 mM imidazole, 100 mM KCl, 5 mM $MgCl_2$, and 5 mM EGTA against 5 mM orthovanadate at 4°C. The polymers formed gradually over the course of 3–4 d. A further 5 mM of vanadate was added to the dialyzing solution at the end of 48 h. This procedure did not result in complete polymerization, but did yield significant numbers of tubular vesicles containing ordered arrays of the Ca ATPase. The most complete polymerization was obtained by adding crystallizing solution directly to SR vesicles suspended in 10 mM imidazole and 0.25 M sucrose. The exact protein concentration was not determined in these preparations, but with negative staining the density of vesicles was roughly equivalent to that of a suspension known to contain 10 mg protein/ml. All procedures were carried out at 4°C and pH 7.0. Two different crystallizing solutions were found to be effective. In the first case 50 μ l of vesicle suspension was diluted with 450 μ l of crystallizing solution (5 mM Na orthovanadate, 100 mM KCl, 10 mM imidazole, 5 mM $MgCl_2$, 0.5 mM EGTA), then pelleted for 10 min using an Eppendorf microfuge and resuspended and incubated in 500 μ l of the crystallizing solution. The ATPase underwent virtually complete polymerization within 24 h, but after 48 h the polymers began to break down and the ordered arrays were less extensive. The other solution that produced extensive polymerization of the ATPase was 10 mM phosphate, 5 mM orthovanadate, 5 mM $MgCl_2$, 1 mM $MnCl_2$, and 5 mM EGTA. 9 ml of this was added to 1 ml of SR vesicle suspension. This treatment produced ordered arrays within several hours, and complete polymerization was induced in virtually all of the nonjunctional SR vesicles within 2 d. These polymers were stable for 10 d with no apparent deterioration.

Scallop SR was isolated as described in Castellani and Hardwicke (1983). A modification of this method was used to isolate crude SR fractions from frog skeletal muscle. Individual sartorius, iliofibularis, and semitendinosus muscles were dissected, spread out, pinned, and bathed in relaxing solution containing either 10 mM phosphate (Castellani and Hardwicke, 1983) or 10 mM HEPES (Endo and Iino, 1980) as the primary buffer for 30 min. The muscles were then soaked in the appropriate relaxing solution containing 50 μ g/ml saponin for 3 h, washed thoroughly in relaxing solution without saponin, finely minced by hand, and homogenized gently (2×1 s). Crude SR fractions were then isolated using centrifugation procedures identical to those described by Herbet et al. (1977).

A crude SR fraction was also obtained from rabbit by mincing fresh skeletal muscle by hand in a solution of 10 mM histidine and 0.25 M sucrose. The tissue was gently homogenized (2×1 s) and SR vesicles were isolated according to the procedure of Herbet et al. (1977).

Some vesicles were prepared for electron microscopy by negatively

staining with 2% uranyl acetate. Other vesicles were freeze dried and rotary shadowed as described in Ferguson et al. (1984). A drop of SR vesicle suspension was placed on a freshly cleaved sheet of mica and the vesicles that had adhered to the mica were washed with solutions of (a) 100 mM ammonium acetate, (b) 100 mM ammonium acetate, followed by 1% uranyl acetate and then water, or (c) 1% uranyl acetate followed by water. The final wash solution was dried to a very thin film, and the mica sheets were frozen in liquid nitrogen and loaded in a double replica holder. The samples were freeze dried at -100 to -110°C under a vacuum of $<2 \times 10^{-6}$ Torr using a Balzer's 400D freeze fracture device (Balzer's, Hudson, NH) and rotary shadowed. The replicas were floated off the mica onto distilled water, cleaned in Clorox, and collected on uncoated grids. Replicas that did not readily detach from the mica were first coated with a thin collodion layer and then detached by briefly soaking in Clorox. Once the replica was deposited on the grid the collodion was removed by dissolving in amyl acetate.

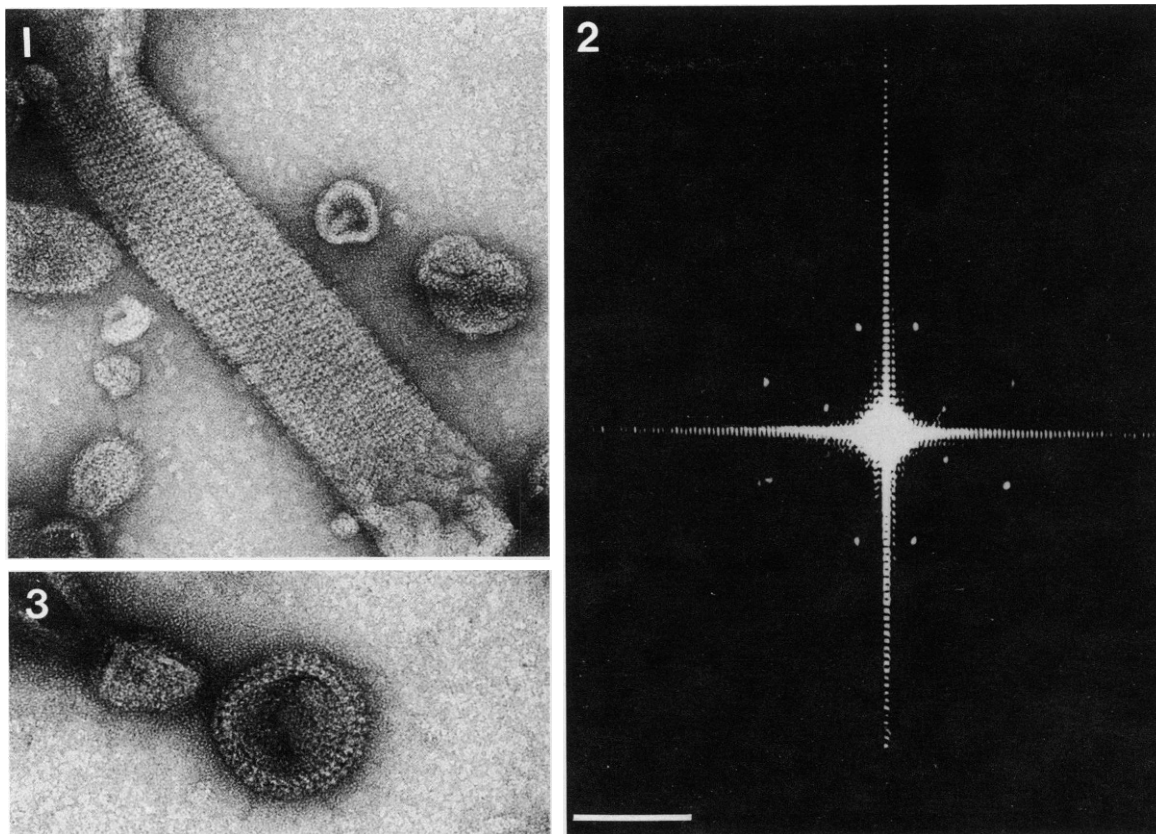
Diffraction patterns of selected areas were obtained using an optical diffractometer modified from Salmon and De Rosier (1981) by Dr. John Weisel, Department of Anatomy, University of Pennsylvania.

RESULTS

Negatively stained images were used as standards for assessing structural preservation in freeze-dried, shadowed vesicles. Fig. 1 is an example of a tubular vesicle in a vanadate-treated, rabbit SR preparation and Fig. 2 is its optical diffraction pattern, which arises from the superimposed top and bottom lattice of the vesicle. The average unit cell dimensions in patterns from four vesicles is $a = 6.5$ nm; $b = 11.3$ nm, with an included angle of 84° . Published filtered images from similar patterns demonstrate that the vesicle surfaces are covered by helically arranged, long rows of paired units (dimers) (Buhle et al., 1983; Castellani and Hardwicke, 1983; Taylor et al., 1984). The two sets of rows forming the superimposed pattern are quite visible in Fig. 1, and our unit cell values are similar to those reported in the literature, except that the ratio of a to b dimensions and the included angle are slightly larger. Lateral projections of the molecules are seen as a fringe at the edges of some spherical vesicles (Fig. 3) and here the regular spacing between rows is clearly visible.

In shadowed preparations only the top surfaces of the vesicles are imaged and even spherical vesicles can be used for direct observation of ATPase disposition and diffraction. Where polymerization is complete most vesicles are entirely occupied by orderly arrays, formed by small shadowed dots. Vesicles that do not contain orderly arrays are of mitochondrial origin and vesicles with only part of the surface occupied by the arrays may have junctional feet and thus belong to junctional SR (see Ferguson et al., 1984). Rare areas representing bare lipid patches appear as depressed surfaces, having a finer grain. Two such patches are illustrated in the accompanying paper (Franzini-Armstrong and Ferguson, 1985). Occasionally, areas of nonpolymerized ATPase are also seen at the ends of tubular vesicles. In crude SR fractions isolated from rabbit white skeletal muscle using the method of Herbet et al. (1977), the great majority of vesicles belong to longitudinal SR and are covered by polymerized ATPase.

The effect of different preparative procedures on the

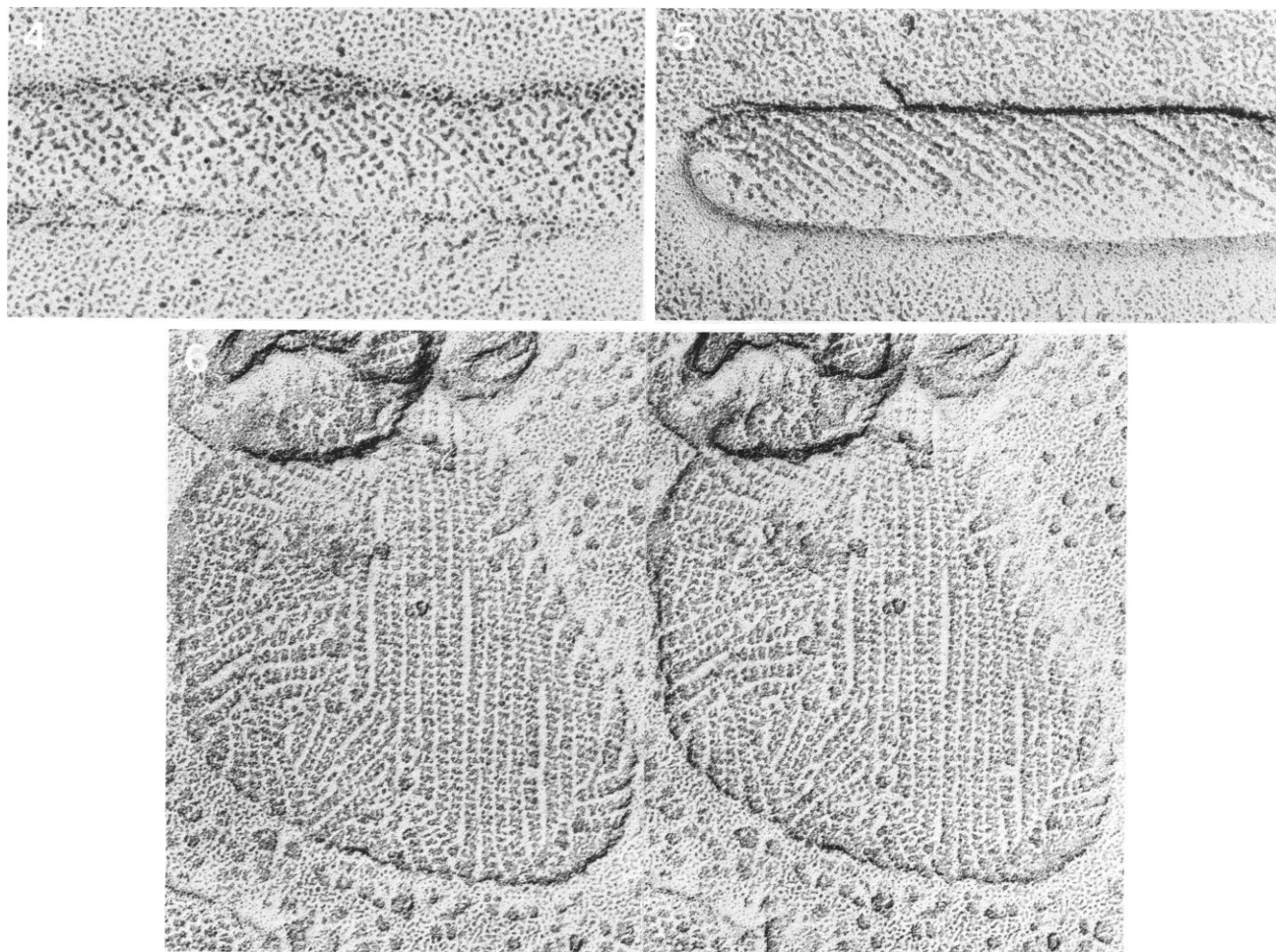


FIGURES 1-3 *Fig. 1:* Negatively stained image of a tubular rabbit SR vesicle after treatment with orthovanadate. The crosshatched pattern is produced by the superposition of dimer rows from front and back sides of the vesicle. $\times 155,000$. *Fig. 2:* Optical diffraction pattern of a selected area from Fig. 1. Reflections from top and bottom patterns are visible. The two unit cells are 6.4×10.3 and 6.3×10.5 nm, respectively. The bar represents a reciprocal lattice spacing of 6 nm^{-1} . *Fig. 3:* A round vesicle from the same sample, which is also polymerized. At the edges of the vesicles the separations between rows of dimers is clearly visible. $\times 275,000$.

appearance of ATPase in shadowed replicas was studied in two samples: (a) a sample of native scallop SR (Figs. 4 and 5) and (b) a vanadate-treated sample of rabbit SR in which polymerization, as judged by negative staining, was complete. In both cases treatment with uranyl acetate results in a more complete preservation of orderly arrays: more extensive areas of polymerization are observed, and the order within the arrays is greater (Figs. 4-6). Complete and quite orderly polymers are present over replicated vesicle surfaces after treatment with uranyl acetate, whether preceded by a wash in 100 mM ammonium acetate or not. Treatment with ammonium acetate alone results in variable preservation of the polymers. In some vesicles (Fig. 4) the arrangement of individual units is disturbed; in others the overall pattern is lost. Since ammonium acetate does not result in disorder when followed by uranyl acetate, we conclude that the problem lies in the freezing. Uranyl acetate stabilizes the polymers so that they are not distorted during the relatively slow freezing obtained by immersion in liquid nitrogen. This observation is consistent with the fact that freezing and thawing of a vanadate-treated vesicle suspension results in some disruption of the pattern.

Areas containing highly ordered arrays are found both on elongated cylindrical vesicles (of the type used for image filtering after negative staining), and on vesicles that maintain the original variable shape (see also Buhle et al., 1984). In the latter, polymerization into long chains must start from different centers simultaneously, since groups of chains run in different directions (Fig. 6).

The regular patterns within well-ordered arrays consist of chains of two closely spaced dots separated by shadow-free strips (Figs. 6, 7, 11, and 12). The most ordered areas were used to compare shadowed and negatively stained images. This was done in two ways: (a) we marked the position of stain, excluding units, in published density maps from negatively stained images on an acetate sheet and superimposed the pattern over images of shadowed vesicles at the same magnification. Over a short distance a one-to-one relationship exists between units in the shadowed replicas and those in the filtered images. Over longer distances the patterns gradually diverge, but considering that the replica images are not averaged and are restricted to the less favorable top surface of the vesicles, the spatial correspondence is quite good. Since units in the filtered images have been interpreted as ATPase monomers, we

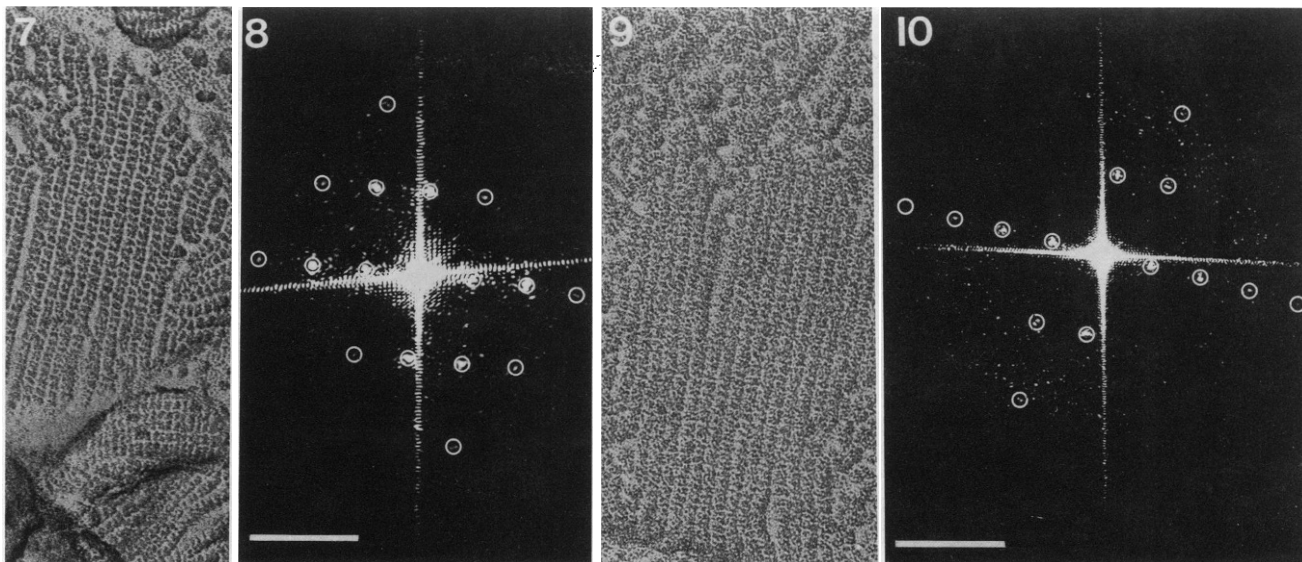


FIGURES 4–6 *Figs. 4 and 5:* Rotary shadowed replicas of tubular vesicles from scallop muscle. Fig. 4 was treated with ammonium acetate, Fig. 5 with ammonium acetate followed by uranyl acetate. Both surfaces are covered by double rows of dots, each dot representing the location of an ATPase molecule. Note that the disposition is more regular in Fig. 5. $\times 285,000$. *Fig. 6:* Stereo pair of a vanadate treated rabbit vesicle. The tilt has been exaggerated to emphasize the difference in position of the shadowed ATPase heads and of the lipid background. This is particularly visible at the edges of the vesicle. Rows of polymerized ATPase form groups with different orientations and variable distances. $\times 198,000$, tilt $\pm 10^\circ$.

identify each shadowed dot in images such as Figs. 6, 11, and 12 as a monomer, and a set of shadowed dots, sometimes fused into a single line, as a dimer. (b) Optical diffraction patterns were obtained from the most orderly areas. Figs. 7–10 show details of two vesicles and diffraction patterns from selected areas. Notice that in Fig. 7 the dimeric disposition of subunits is quite clear to the eye, while in Fig. 9, which has a lighter shadow, the rows are visible but individual units are hidden in the grain of the shadow. Nonetheless, both images give excellent diffraction patterns. From selected areas of round or oval vanadate-treated rabbit vesicles, unit cells have the following average dimensions: $a = 6.5$ nm; $b = 10.7$ nm (from 10 patterns); the included angle varies between 76° and 90° (average 85.5°). From diffractions of four photographs of tubular scallop vesicles we obtain the following average values: $a = 5.8$ nm; $b = 10.9$ nm, angle 78.8° . As is the case for our negatively stained vesicles, the ratio of a and b dimensions is slightly larger than that in the literature.

From the best images we obtain reflections up to the fourth order of a spacing of ~ 10 nm in the direction perpendicular to the rows (Fig. 10), and to the second order of an approximately 6-nm spacing along the rows (Fig. 8). Overall, these images show a preservation equivalent to that following negative staining and sufficient resolution to detect single ATPase molecules. The diffraction patterns confirm that the disposition of polymers over nonelongated vesicles is the same as in tubular ones.

In the selected areas that give good diffraction patterns the center-to-center separation between rows is constant within the area, but it varies from one vesicle to the other. In most cases the spacing was between 10.1 and 10.7 nm, but in two cases (one from vanadate-treated rabbit and the other from scallop) it was considerably larger (13.2 and 15.1 nm, respectively). The scallop spacing was not included in the average data given above because it was from a round rather than a tubular vesicle. In less orderly areas the distance between rows is considerably more



FIGURES 7-10 Details of two vesicles and optical diffraction patterns from selected areas. Reflections that index on a slightly skewed lattice of ~ 7 and 11 nm^{-1} are circled. Notice that both patterns show a second-order reflection of the 7-nm spacing, and up to third- and fourth-order reflections of the 11-nm spacing are visible in Figs. 8 and 10, respectively. The bars represent reciprocal lattice spacings of 6 nm^{-1} . A fourth order was also present in a Fourier transform calculated from the digitized image of Fig. 9 by Dr. John Murray (University of Pennsylvania). Figs. 7 and 9, $\times 186,000$.

variable (Fig. 6). To determine the narrowest possible separation between adjacent rows, we measured center-to-center spacings in areas selected from stereo micrographs for their flatness. This excluded spacing variations simply due to tilt. Out of 23 areas thus selected, five had spacings of $<10 \text{ nm}$, and the minimum spacing measured was 8.9 nm . We did not determine the widest spacing, but for short distances the rows can be separated by a fairly wide gap. Stereo pairs (Fig. 6) show that the background between the rows is at a lower level, and thus presumably the surface of the lipid bilayer is exposed at those sites.

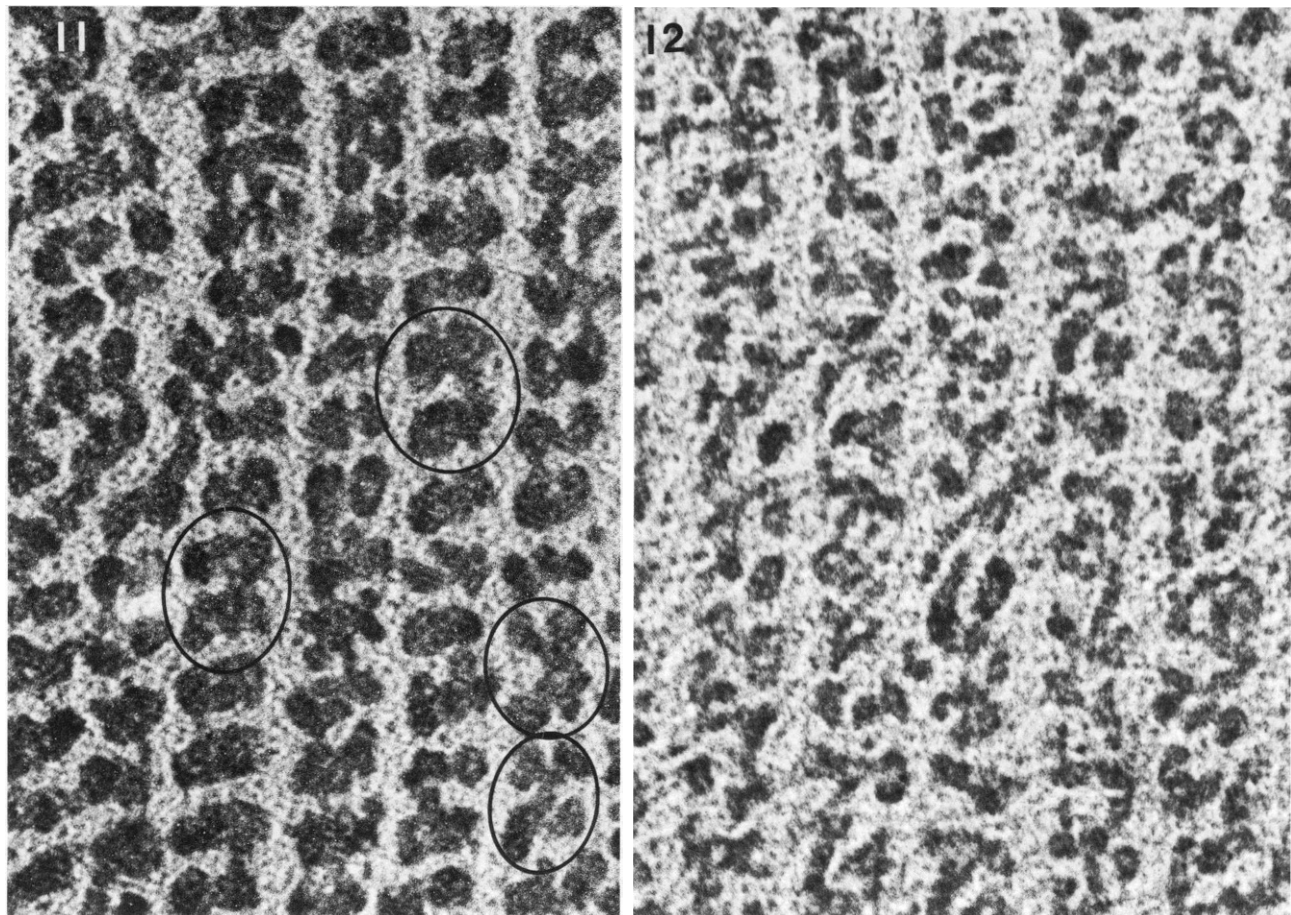
The appearance of the chains and of the individual units depends on the amount and direction of platinum deposition. Figs. 11 and 12 compare two replicas with heavier (Fig. 11) and lighter (Fig. 12) shadows. Individual subunits are more clearly separated in Fig. 12, but dimers are most obviously delineated in Fig. 11. A second effect of shadowing is the enhancement of either the dimeric arrangement (Figs. 11 and 13), or the chain arrangement (Fig. 14) of the units. Even though the shadow was applied while rotating the specimen, vesicles are often asymmetrically shadowed (Figs. 13 and 14), possibly as a result of a slight tilt of the mica sheet relative to the platinum source. Moving from the top to the bottom of the image, the shadow becomes progressively lighter. At the top the chains are a single structure, farther down dimers are distinct, and towards the bottom individual molecules are clearly resolved.

The appearance of individual units and dimers is also quite variable, in part as function of the amount of platinum deposited. Subunits may be either single dots (mostly in very lightly shadowed replicas), or circles and

C-shapes. Dimers may have separate units, or more frequently form dumbbell or cylindrical particles, the two monomers being linked by a bridge. A decidedly heavier platinum deposition results in lack of resolution of the units, and the only visible pattern is that of wide strips, separated by shadow-free intervals. These different appearances can arise from quite small variations in platinum thickness: They were observed within samples from the same run, which differed from each other only in being mounted at varying distances from the center of rotation of the specimen holder.

Other variations in the appearance of dimers and tetramers (groups of two adjacent dimers) are probably due to a slight distortion of the heads and are more prominent in vesicles not preserved with uranyl acetate. We describe these here because they serve as a basis for the identification of tetramers in nonorderly ATPase distributions. The variations include: (a) U-shaped tetramers, in which the platinum shadow bridges four subunits together on three sides (circle, Fig. 11); (b) X-shaped tetramers, in which the platinum bridges the subunits across the center of the tetramer (circle, Fig. 11); and most frequently (c) tetramers in which the two dimers have a dumbbell or rod shape, and are separated from each other by a clear space.

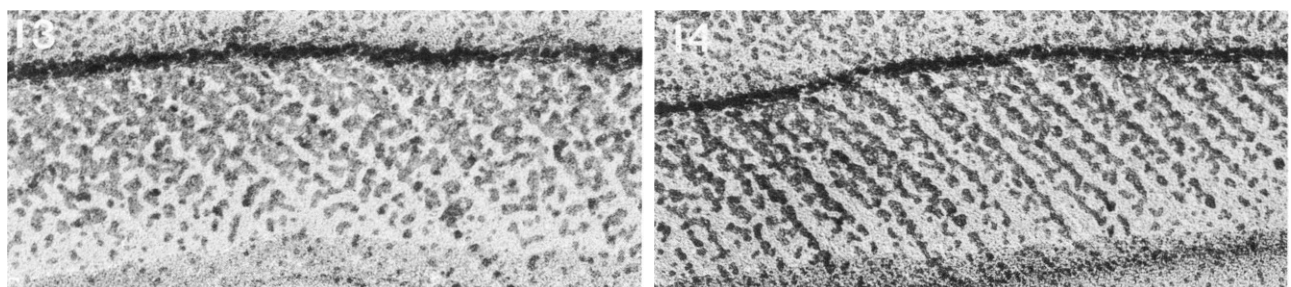
Scallop vesicles have extensively polymerized ATPase without being exposed to vanadate and phosphate, provided they are isolated by gentle homogenization (Castellani and Hardwicke 1983, 1985, and this paper). We wanted to verify whether similar isolation conditions (see Methods) would result in polymerized vesicles when used in muscles from vertebrates (rabbit and frog). In general gently isolated vesicles are larger than those from standard



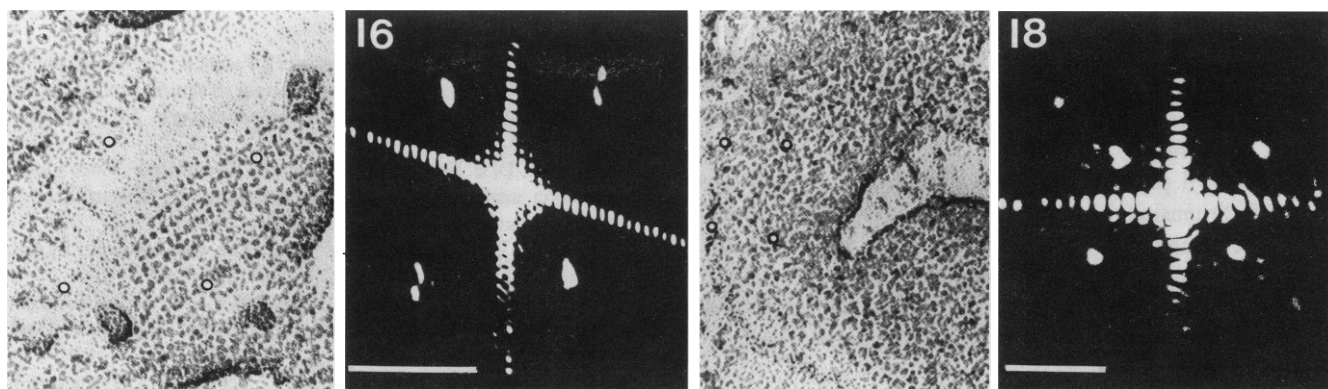
FIGURES 11 and 12 *Fig. 11:* Detail of a vanadate-treated rabbit vesicle. The dimeric arrangement of subunits is emphasized by bridges joining the two subunits of each monomer. Groups of two dimers (tetramers) with special appearances have been circled: Two U-shaped tetramers are near the center, two adjacent X-shaped tetramers are near the bottom. $\times 1,400,000$. *Fig. 12:* Image from a vesicle similar to that in Fig. 13. The dimeric arrangement is less immediately obvious, but this area gave a quite good diffraction pattern. Individual molecules show fine structural details in this lighter shadow, but these may simply be decoration effects of the shadow. $\times 1,400,000$.

isolation procedures, and many have tubular shapes. The majority of the vesicles have a random distribution of shadowed ATPase over their surface. However, several vesicles have limited areas of a more regular pattern (Figs. 15 and 17). Selected areas from 12 rabbit SR vesicles were sufficiently orderly to produce diffraction patterns with first (and in three cases second) order reflections (Figs. 16

and 18). 12 vesicles gave measurable patterns showing a skewed lattice with average dimensions of 5.1 and 6.5 nm^{-1} and an average angle of 79° . Both dimensions were somewhat variable, the ranges being $4.4\text{--}5.7$ and $6.0\text{--}7.1 \text{ nm}^{-1}$ for the two dimensions. This disposition is different from the dimeric arrangement seen in uranyl acetate-treated scallop vesicles. However, these rabbit SR vesicles were not



FIGURES 13 and 14 Tubular vesicles from isolated scallop SR illustrating that slight variations in shadow may account for the different appearances of Figs. 11 and 12. The shadow is heaviest at the top and progressively lighter toward the bottom. Correspondingly, individual units become more distinct. In Fig. 13 the dimeric arrangement is enhanced; in Fig. 14 the disposition in rows is visible. $\times 450,000$.



FIGURES 15–18 Limited orderly arrangement of ATPase in vesicles isolated by gentle homogenization of rabbit skeletal muscle (Figs. 15 and 17) and diffraction patterns obtained from the areas outlined by the white dots (Figs. 16 and 18). The lattice has dimensions of $\sim 5 \times 6 \text{ nm}^{-1}$. The bar represents a reciprocal lattice spacing of 5 nm^{-1} . In Fig. 18 a second-order reflection of the 6-nm spacing is visible. Both vesicles are quite large and have an elongated shape. Figs. 15 and 17, $\times 310,000$ and $205,000$, respectively.

stabilized with uranyl acetate before freezing and similarly treated scallop samples occasionally contained orderly, nondimeric patterns.

Vesicles that were isolated from frog muscle with phosphate buffers also showed regular patterns, but we were only able to obtain one diffraction pattern. In the other vesicles the dots formed curving lines.

DISCUSSION

This paper demonstrates that freeze-drying (after stabilization with uranyl acetate) and shadowing result in sufficient preservation and resolution to allow identification of the heads of individual ATPase molecules on the cytoplasmic surface of isolated SR vesicles. The approach has the advantage of allowing direct visualization of a single surface, so that small polymerized patches, nontubular vesicles, and disorderly arrangements can be studied (see Franzini-Armstrong and Ferguson, 1985 for the latter). Our preparations give slightly higher values for the ratio of the unit cell dimensions and for included angle than those in the literature (Buhle et al., 1983; Castellani and Hardwicke, 1983; Taylor et al., 1984), but this is likely due to flattening of the vesicles during freeze drying.

Slightly heavier shadowing accentuates the dimeric arrangement of ATPase by joining the two subunits of each dimer. It is possible that this emphasizes a bridge between the two adjacent ATPases which is located on the cytoplasmic side of the vesicle (Castellani et al., 1985). With lighter shadows individual heads have variable appearances, including ring and C-shapes, as first described by Peracchia et al. (1984). However, since the dimensions of the head are close to the size of the platinum grain (Fowler and Aeby, 1983), for the moment we conclude that these variations may be an effect of decoration.

A brief treatment with 1% uranyl acetate enhances the preservation of ultrastructural detail of membrane-associated proteins, limiting the amount of distortion during

freezing and/or freeze drying (see also Ferguson et al., 1984). This use of uranyl salts for “fixing” has come into prominence with recent work on muscle filaments (Stewart et al., 1981) but has also been previously used in the study of isolated membranes (Brown and Shorey, 1963).

Two observations on vanadate-induced order confirm the concept (Buhle et al., 1984) of polymerization of the ATPase in the form of long rows of dimers, which secondarily acquire a constant separation and impose a tubular shape to the vesicles: (a) complete polymerization can occur on the surface of irregularly shaped vesicles and (b) spacing of dimers along the rows is quite constant, but separation between rows can be variable.

It is interesting that rabbit SR ATPase, polymerized in the presence of vanadate, and the naturally occurring orderly arrays in scallop SR vesicles have molecular dispositions that are identical at the level of resolution obtained using negative staining (compare Taylor et al., 1984 and Buhle et al., 1984 with Castellani and Hardwicke, 1983). Vanadate stabilizes the ATPase in a particular state of the catalytic cycle (Inesi et al., 1980), thereby inhibiting the pump. The structural effects can be reversed by greatly increasing the concentration of free Ca^{2+} (Medda and Hasselbach, 1983). On the other hand, scallop muscle SR vesicles bearing polymerized ATPase are fully functional and can be obtained by isolation in Ca^{2+} -free solutions, both in the presence and absence of phosphate (Castellani and Hardwicke, 1983, 1985).

The Na,K ATPase can also form polymers. These have several different configurations, one of which (Zampighi et al., 1984; Herbert et al., 1982) is a dimeric arrangement with unit cells virtually identical to those of the Ca ATPase. In addition, the Na,K ATPase forms monomeric arrays with unit cell dimensions of $5 \times 6 \text{ nm}$. We have found that SR vesicles, obtained by gentle homogenization of vertebrate muscles, contain occasional patches of polymerized ATPase with spacings comparable to that of the monomeric Na,K ATPase disposition. However, since the

shadowing does not give detail of the molecular shape, we cannot yet tell whether these orderly arrangements are truly monomeric (i.e., with all units facing in one direction), or are distorted dimeric arrangements (i.e., with paired units facing each other). The Na,K ATPase also forms a third pattern, interpreted as dimeric, which has unit cell dimensions of 5.5×16.1 nm (Mohraz and Smith, 1984). A comparable arrangement has not been described in Ca ATPase, but we have found two orderly areas with 13 and 15 nm spacings between rows. We have also measured spacings as small as 8.9 nm between the rows, although this is rare.

In addition to the calcium pump protein, SR membranes contain a 53,000-mol-wt glycoprotein, present in a high molecular ratio to the ATPase (1:1.5, Michelak et al., 1980). The glycoprotein has been characterized and identified as an intrinsic membrane protein (Campbell and MacLennan, 1981). The location of the glycoprotein is still somewhat uncertain. Jorgensen et al. (1981) suggest that it is restricted to the region of the terminal cisternae, while Campbell et al. (1980, 1984) find it in both heavy and light SR fractions. Considering that both the alpha and beta subunits of the Na,K ATPase, with a combined molecular weight of 150,000 d, can fit into an array with unit cell dimensions virtually identical to those of the Ca ATPase, it is likely that sufficient space for the 53,000-mol-wt glycoprotein is available within polymerized Ca ATPase areas.

Discounting junctional SR, practically the entire surface of vanadate-treated rabbit SR vesicles is covered by polymerized ATPase. Using the unit cell dimensions given in the literature and in this paper, we calculate that the surface density of the polymerized ATPase molecules is $31\text{--}35,000/\mu\text{m}^2$. The density in native SR should be similar to this. Actual counts using freshly isolated rabbit SR vesicles (Franzini-Armstrong and Ferguson, 1985) indeed confirm this expectation. An estimate of the extent of polymerization, obtained by counting the proportion of negatively stained vanadate-treated vesicles having orderly arrays (Dux and Martonosi, 1984), reached similar conclusions.

We are grateful to Dr. John Weisel for the use of his optical diffractometer and Dr. John Murray for extensive advice and for calculating Fourier transforms from digitized images for us. The diffractometer was built with funds from the Biomedical Research Support Grant (Medical School and University of Pennsylvania), Nos. RR07083-17 and 2S07-RR-05415. We thank Mrs. D. Appelt-Byler for expert technical and photographic help, and Mr. D. Wray for microscope maintenance.

This work was supported by grants from the National Institutes of Health (HL 15835-11) to the Pennsylvania Muscle Institute, and from National Science Foundation (PCM82-02516) and the Muscular Dystrophy Association to Dr. C. Cohen. D. G. Ferguson is a fellow of the Alberta Heritage Foundation for Medical Research and L. Castellani is a fellow of the The Charles A. King Trust.

Received for publication 21 November 1984 and in final form 9 May 1985.

REFERENCES

- Blaisie, J. K., L. Herbette, D. H. Pierce, D. Pascolini, A. Scarpa, and S. Fleischer. 1982. Static and time resolved structural studies of the CaATPase of isolated sarcoplasmic reticulum. *Ann. NY Acad. Sci.* 402:478-484.
- Brady, G. W., D. B. Fein, M. E. Harder, and G. Meissner. 1982. Liquid diffraction analysis of sarcoplasmic reticulum. II. Solvent electron contrast variation. *Biophys. J.* 37:637-645.
- Brown, A. D., and C. D. Shorey. 1963. The cell envelopes of two extremely halophilic bacteria. *J. Cell Biol.* 18:681-689.
- Buhle, E. L., B. E. Knox, and U. Aebi. 1983. Structural analysis of crystalline Ca^{2+} transport ATPase vesicles. *Proc. 41st Annu. Meet. EMSA.* 636-637.
- Buhle, E. L., B. E. Knox, E. Serspersu, and U. Aebi. 1984. The structure of the Ca^{2+} ATPase as revealed by electron microscopy and image processing of ordered arrays. *J. Ultrastruct. Res.* 85:186-203.
- Campbell, K. P., and D. H. MacLennan. 1981. Purification and characterization of the 53,000-dalton glycoprotein from the sarcoplasmic reticulum. *J. Biol. Chem.* 256:4626-4632.
- Campbell, K. P., C. Franzini-Armstrong, and A. E. Shamoo. 1980. Further characterization of light and heavy sarcoplasmic reticulum vesicles. Identification of the "sarcoplasmic reticulum feet" associated with heavy sarcoplasmic reticulum vesicles. *Biochim. Biophys. Acta.* 602:97-116.
- Campbell, K. P., C. Bomgaars, D. H. Denney, and A. Sharp. 1984. Production and characterization of monoclonal antibodies directed against the cytoplasmic face of the sarcoplasmic reticulum. *Biophys. J.* (2, Pt. 2) 45:4a. (Abstr.)
- Castellani, L., and P. M. D. Hardwicke. 1983. Crystalline structure of sarcoplasmic reticulum from scallop. *J. Cell Biol.* 97:557-561.
- Castellani, L., P. M. D. Hardwicke, and P. Vibert. 1985. Dimer ribbons in the three dimensional structure of sarcoplasmic reticulum. *J. Mol. Biol.* In press.
- Dean, W. L., and C. Tanford. 1977. Reactivation of lipid depleted Ca^{2+} ATPase by nonionic detergent. *J. Biol. Chem.* 252:3551-3553.
- Dupont, Y., S. C. Harrison, and W. Hasselbach. 1973. Molecular organization in the sarcoplasmic reticulum membrane studied by x-ray diffraction. *Nature (Lond.)* 244:555-557.
- Dux, L., and A. Martonosi. 1983a. Two dimensional arrays of proteins in sarcoplasmic reticulum and purified Ca^{2+} ATPase vesicle treated with vanadate. *J. Biol. Chem.* 258:2599-2603.
- Dux, L., and A. Martonosi. 1983b. The regulation of ATPase-ATPase interactions in sarcoplasmic reticulum membrane. I. The effects of Ca^{2+} , ATP, and inorganic phosphate. *J. Biol. Chem.* 258:11896-11902.
- Dux, L., and A. Martonosi. 1984. Membrane crystals of Ca^{2+} ATPase in sarcoplasmic reticulum of fast and slow skeletal and cardiac muscles. *Eur. J. Biochem.* 141:43-49.
- Endo, M., and M. Iino. 1980. Specific perforation of muscle cell membranes with preserved SR functions by saponin treatment. *J. Muscle Res. Cell Motil.* 1:89-100.
- Farley, R. A. 1983. Identification of hydrophobic regions of the calcium transport ATPase from sarcoplasmic reticulum after photochemical labeling with adamantane diazine. *Int. J. Biochem.* 15:1423-1427.
- Ferguson, D. G., H. A. Schwartz, and C. Franzini-Armstrong. 1984. Subunit structure of junctional feet in triads of skeletal muscle. A freeze drying rotary shadow study. *J. Cell Biol.* 99:1735.
- Franzini-Armstrong, C., and D. G. Ferguson. 1985. Density and disposition of Ca^{2+} -ATPase in sarcoplasmic reticulum membrane as determined by shadowing techniques. *Biophys. J.* 48:607-615.
- Fowler, W. E., and U. Aebi. 1983. Preparation of single molecules and supramolecular complexes for high resolution metal shadowing. *J. Ultrastruct. Res.* 83:319-334.
- Hardwicke, P. M. D., and N. M. Green. 1974. The effect of delipidation on the adenosine triphosphatase of sarcoplasmic reticulum. Electron microscopy and physical properties. *Eur. J. Biochem.* 42:183-193.

- Hasselbach, W., and L.-G. Elfvin. 1967. Structural and chemical asymmetry of the calcium transporting membranes of the sarcotubular system as revealed by electron microscopy. *J. Ultrastruct. Res.* 17:598–622.
- Herbert, H., P. L. Jorgensen, E. Skriver, and A. B. Maunsbach. 1982. Crystallization patterns of membrane bound ($\text{Na}^+ + \text{K}^+$)-ATPase. *Biochim. Biophys. Acta.* 689:571–574.
- Herbette, L., J. Marquardt, A. Scarpa, and J. K. Blasie. 1977. A direct analysis of lamellar X-ray diffraction from hydrated oriented multi-layers of fully functional sarcoplasmic reticulum. *Biophys. J.* 20:245–277.
- Hidalgo, C., and Ikemoto, N. 1977. Disposition of proteins and amino-phospholipids in the sarcoplasmic reticulum membrane. *J. Biol. Chem.* 252:8446–8454.
- Ikemoto, N. 1982. Structure and function of the calcium pump protein of sarcoplasmic reticulum. *Annu. Rev. Physiol.* 44:297–317.
- Ikemoto, N., F. A. Sreter, A. Nakamura, and J. Gergely. 1968. Tryptic digestion and localization of calcium uptake and ATPase activity in fragments of sarcoplasmic reticulum. *J. Ultrastruct. Res.* 23:216–232.
- Inesi, G., and D. Scales. 1974. Tryptic cleavage of sarcoplasmic reticulum protein. *Biochemistry.* 13:3298–3306.
- Inesi, G., M. Kurzmack, R. Nakamoto, L. de Meis, and S. Bernhard. 1980. Uncoupling of calcium control and phosphohydrolase activity in sarcoplasmic reticulum vesicles. *J. Biol. Chem.* 255:6040–6043.
- Jilka, R. L., A. Martonosi, and T. W. Tillack. 1975. Effect of purified ($\text{Mg}^{2+} + \text{Ca}^{2+}$) activated ATPase of sarcoplasmic reticulum upon the passive Ca^{2+} permeability and ultrastructure of phospholipid vesicles. *J. Biol. Chem.* 250:7511–7524.
- Jorgensen, A. O., P. Daly, K. P. Campbell, and D. H. MacLennan. 1981. Localization of the 53,000 dalton intrinsic glycoprotein of the sarcoplasmic reticulum in adult rat skeletal muscle. *J. Cell Biol.* 91:345a (Abstr.)
- Le Maire, M., J. V. Moller, and C. Tanford. 1976. Retention of enzyme activity by detergent solubilized sarcoplasmic Ca^{2+} ATPase. *Biochemistry.* 15:2336–2342.
- MacLennan, D. H. 1970. Purification and properties of an adenosine triphosphatase from sarcoplasmic reticulum. *J. Biol. Chem.* 245:4508–4513.
- MacLennan, D. H., P. Seeman, G. H. Iles, and C. C. Yip. 1971. Membrane formation by the adenosine triphosphatase of sarcoplasmic reticulum. *J. Biol. Chem.* 246:2702–2710.
- Martonosi, A., and T. J. Beeler. 1983. Mechanism of Ca^{2+} transport by sarcoplasmic reticulum. *Handb. Physiol.* 417–487.
- Medda, P., and W. Hasselbach. 1983. The vanadate complex of the calcium-transport ATPase of the sarcoplasmic reticulum, its formation and dissociation. *Eur. J. Biochem.* 137:7–14.
- Meissner, G., and S. Fleischer. 1971. Characterization of sarcoplasmic reticulum from skeletal muscle. *Biochim. Biophys. Acta.* 241:356–361.
- Michalak, M., K. P. Campbell, and D. H. MacLennan. 1980. Localization of the high affinity calcium binding protein and an intrinsic glycoprotein in sarcoplasmic reticulum membranes. *J. Biol. Chem.* 255:1317–1326.
- Mohraz, M., and P. R. Smith. 1984. Structure of (Na^+, K^+)-ATPase as revealed by electron microscopy and image processing. *J. Cell Biol.* 98:1836–1841.
- Moller, J. V., K. E. Lind, and J. P. Andersen. 1980. Enzyme kinetics and substrate stabilization of detergent-solubilized and membranous ($\text{Ca}^{2+} + \text{Mg}^{2+}$) activated ATPase from sarcoplasmic reticulum. Effect of protein-protein interactions. *J. Biol. Chem.* 255:1912–1920.
- Moller, J. V., J. P. Andersen, and M. LeMaire. 1982. The sarcoplasmic reticulum Ca^{2+} ATPase. *Mol. Cell. Biochem.* 42:83–107.
- Peracchia, C., L. Dux, and A. N. Martonosi. 1984. Crystallization of intramembrane particles in rabbit sarcoplasmic reticulum vesicles by vanadate. *J. Musc. Res. Cell Motil.* 5:431–442.
- Racker, E. 1972. Reconstitution of calcium pump with phospholipids and a purified Ca^{2+} -adenosine triphosphatase from sarcoplasmic reticulum. *Biochim. Biophys. Acta.* 363:159–163.
- Saito, A., C. T. Wang, and S. Fleischer. 1978. Membrane asymmetry and enhanced ultrastructural detail of sarcoplasmic reticulum revealed with use of tannic acid. *J. Cell Biol.* 79:601–616.
- Salmon, D., and D. De Rosier. 1981. A surveying optical diffractometer. *J. Microsc. (Oxf.)* 123:239–247.
- Scales, D., and G. Inesi. 1976. Assembly of ATPase protein in sarcoplasmic reticulum membranes. *Biophys. J.* 16:735–751.
- Stewart, M., R. W. Kensler, and R. J. C. Levine. 1981. Structure of limulus telson muscle thick filaments. *J. Mol. Biol.* 153:781–790.
- Stewart, P. S., and D. H. MacLennan. 1974. Surface particles of sarcoplasmic reticulum membranes. Structural features of the adenosine triphosphatase. *J. Biol. Chem.* 249:985–993.
- Taylor, K., L. Dux, and A. Martonosi. 1984. Structure of the vanadate induced crystals of sarcoplasmic reticulum Ca^{2+} ATPase. *J. Mol. Biol.* 174:193–204.
- Wang, C. T., A. Saito, and S. Fleischer. 1979. Correlation of ultrastructure of reconstituted sarcoplasmic reticulum membrane vesicles with variation in phospholipid to protein ratio. *J. Biol. Chem.* 254:9209–9219.
- Zampighi, G., J. Kyte, and W. Freytag. 1984. The structural organization of (Na^+, K^+) ATPase in purified membranes. *J. Cell Biol.* 98:1851–1864.